

# Polymer self-diffusion in NaI-poly(ethylene oxide) electrolytes

En S. Wu

Department of Physics, University of Maryland Baltimore County,  
Catonsville, MD 21228, USA

and John H. Shibata\* and Francis W. Wang

Polymers Division, National Institute of Standards and Technology,  
Gaithersburg, MD 20899, USA

(Received 18 February 1991; revised 9 May 1991; accepted 17 May 1991)

Using the technique of fluorescence recovery after photobleaching we have measured the self-diffusion coefficients ( $D$ ) of poly(ethylene oxide) (PEO) in NaI-PEO electrolytes. From the temperature dependence of the  $D$  values, the activation energy of self-diffusion was obtained. It has the same salt concentration dependence as the activation energy of ionic conductivity, suggesting that polymer segmental mobility is essential for ion transport in NaI-PEO electrolytes. The PEO diffusion rate was reduced significantly at low salt concentration, but raising the NaI concentration beyond 6 mol% resulted in only slight changes in  $D$  values. The concentration dependence of  $D$  was interpreted in terms of the interactions between PEO and sodium ions. From the response of  $D$  and the immobile fraction of PEO molecules to temperature and composition changes, several features in the NaI-PEO phase diagram were elucidated.

(Keywords: fluorescence recovery after photobleaching; self-diffusion; poly(ethylene oxide); electrolytes)

## INTRODUCTION

Solutions of alkali metals in polymeric materials, such as poly(ethylene oxide) (PEO) have been extensively studied in the last decade<sup>1-3</sup>, mainly because of their potential application as electrolytic media in high energy density batteries. However, details of the mechanism of electric conduction remain elusive. Over the past few years, through many careful measurements, the early theory that conduction is due to ionic migrations inside helical NaI-PEO complexes<sup>4,5</sup> has been replaced by a thermodynamics-based approach, in which the ionic conductivity is interpreted in terms of several interrelated factors, among them, the ionic interactions<sup>6-8</sup>, the local dynamics of the polymer segments<sup>9-13</sup> and the phase structures of the electrolytes<sup>14-17</sup>. The relative importance of these factors in accounting for the observed ionic conductivity is not totally clear and probably varies for different electrolytes, but the existing data strongly suggest that ionic conduction takes place mainly in the amorphous phase and the dominating factor is the mobility of the polymer chain segments. The transport of ions is accompanied by polymer segmental motion, as a result, the ionic conductivity increases with the increase in polymer chain mobility. Since information on polymer chain mobility can be obtained from the self-diffusion of polymer molecules, it would be useful to study the self-diffusion of PEO in NaI-PEO electrolytes.

The self-diffusion of a polymer chain is determined by the local viscosity around the chain segments and also by the hindrance due to the entanglements among

different chains<sup>18-21</sup>. Local viscosity is essentially a measure of the free volume of the system. As the temperature increases more free volume is created, leading to higher chain segmental mobility and lower local viscosity. For ions dissolved in the polymer, the increase in free volume provides additional pathways for ions to diffuse, thus raising the ionic conductivity. Therefore, polymer diffusion and ionic conductivity are expected to exhibit similar temperature dependence. Recently, Fauteux *et al.* measured the ionic conductivity in NaI-PEO electrolytes as a function of temperature<sup>14</sup>, from which the activation energy ( $E_a$ ) of ionic conduction was obtained. In contrast, we have determined the  $E_a$  of diffusion from the temperature dependence of PEO diffusion coefficients. By comparing the results from these two studies, the role of segmental mobility in ionic conduction can be examined.

Long chain polymers may entangle with each other to form an entangled network. For a polymer molecule to diffuse over a macroscopic distance, it must disentangle itself from the network, and such disentanglement has been demonstrated to be the dominating factor in polymer self-diffusion<sup>20,21</sup>. In NaI-PEO electrolytes, sodium ions ( $\text{Na}^+$ ) may interact with oxygen atoms on the polymers to form a transient network. Such an interaction is dynamic in nature, a quantitative assessment of its effect on diffusion is difficult and is a subject under intensive investigation<sup>22,23</sup>. Nevertheless, the associations of  $\text{Na}^+$  and oxygen atoms have the same qualitative effect as forming a transient entangled network<sup>22-25</sup> that may effectively reduce the rate of PEO diffusion. This will be examined in this work by studying the dependence of PEO diffusion on NaI concentration.

\* Present address: Department of Chemistry, University of Tennessee, Knoxville, TN 37996, USA

Experimentally, we used the technique of fluorescence recovery after photobleaching (FRAP) to measure the diffusion coefficient ( $D$ ) of fluorescently labelled PEO<sup>26-28</sup>. In addition to determining  $D$  as a function of temperature and NaI concentration, we also measured the fraction of immobile PEO molecules, which is a direct measurement of the amount of PEO in the crystalline state. From the response of  $D$  and the fraction of PEO in the crystalline state to variations in temperature and salt concentration, information on the NaI-PEO phase diagram has also been obtained.

## MATERIALS AND METHODS

**Materials\*.** The PEO (molecular weight 8650;  $M_w/M_n = 1.10$ ) was obtained from Polysciences (Warrington, PA, USA). The fluorescent chromophore 6-(*N*-(7-nitrobenz-2-oxa-1,3-diazol-4-yl)amino)hexanoic acid (NBD hexanoic acid) was obtained from Molecular Probes (Eugene, OR, USA). Anhydrous h.p.l.c. grade dimethyl formamide (DMF) stored with added hygroscopic molecular sieve particles was used without further purification. Spectral grade NaI was obtained from Sigma. Acetonitrile and other solvents were from VWR and were reagent grade.

**Fluorescence labelling.** NBD hexanoic acid was attached to the terminal OH group in PEO by esterification following the procedure of Cuniberti and Perico<sup>29</sup>. DMF was used as the solvent in our reaction mixture in place of toluene due to the observed insolubility of NBD hexanoic acid in toluene. The final product was determined to be free of unbound dye by Fourier transform infra-red spectroscopy and by fluorescence measurements on fractions eluted from g.p.c. In addition, thermal analysis and g.p.c. measurements on labelled and unlabelled PEO revealed no discernible differences in transition temperatures and molecular weight due to the presence of NBD. Standard fluorescence measurements indicated a maximum of one dye per polymer chain.

**FRAP sample preparation.** Proper amounts of PEO and NaI were mixed in acetonitrile at room temperature. Solutions were concentrated under dry nitrogen, then cast on precleaned microscope slides to form thin films several micrometres thick. Samples were then baked in a vacuum oven at 90°C for 48–72 h to remove the residual solvents. Dry samples were removed from the oven and immediately placed under dry nitrogen. A no. 1 cover slip was placed over the polymer film, and the edges were sealed with fast curing epoxy. Properly sealed samples exhibited consistent and reproducible diffusion results over a period of several months.

Physical properties of crystal forming polymers are frequently dependent on their thermal histories. For consistency, prior to each set of measurements, samples were held at ~90°C for at least 15 min to ensure that the PEO was melted. This was confirmed by the disappearance of birefringence examined under a cross-polarized microscope. The samples were then allowed to cool slowly to the desired temperature in the subsequent measurements.

\* Commercial materials are identified to specify the experimental procedure. Such identification does not imply recommendation or endorsement by the National Institute of Standards and Technology

**FRAP measurements.** Details of the FRAP technique and its application to polymer systems were published previously<sup>26-28</sup>. Samples were placed on a microscope stage thermally regulated to  $\pm 0.8^\circ\text{C}$  by a circulating bath of antifreeze. The temperature was measured by a surface temperature probe in contact with the stage, which has a centre hole ( $3 \times 6 \text{ mm}^2$ ) for transmitted light illumination. The sample within this area is exposed to the ambient environment. As a result, the true temperature of the sample is slightly lower than the reported value.

## RESULTS AND DISCUSSION

### Fluorescence recovery after photobleaching

Two important physical parameters can be obtained from a measured fluorescence recovery curve,  $D$  and the fraction of fluorescence recovery ( $R$ ).  $R$  is defined as

$$R = \frac{F(\infty) - F(t_b)}{F(0) - F(t_b)}$$

where  $F(0)$  and  $F(\infty)$  are the initial and the final fluorescence intensities, respectively, and  $F(t_b)$  is the fluorescence intensity immediately following the photobleaching (which occurs at time  $t_b$ ). In a crystal forming polymer system, the  $R$  value is particularly useful in assessing the crystalline state of the system. In the liquid state where all the molecules are mobile, a FRAP measurement would yield  $R \sim 1$  for a complete fluorescence recovery after photobleaching. On the other hand, a FRAP measurement performed on crystals would yield a low  $R$  value, indicating the presence of a large fraction of molecules which are immobile on the time scale of the measurement. Since the immobile fraction is presumably due to the crystallization of PEO molecules, the observed  $R$  value is a direct measure of the crystalline state of the system. Depending on the sample composition and the temperature, a typical fluorescence recovery curve may fall into one of the following three categories as illustrated in *Figure 1*. In the first case (*Figure 1A*), the recovery curve can be fitted to a theoretical curve for the diffusion of a single species, and the fluorescence recovery is almost complete ( $R \sim 1$ ). These results indicate that only a single fluorescent species is involved in the diffusion process and fluorescent molecules in the illuminated area are completely mobile. In the second case (*Figure 1B*), the recovery curve can be described by the diffusion of a single species, but the recovery is not complete ( $R < 1$ ), indicating that some of the molecules in the probed area are not mobile. In the last case (*Figure 1C*), the measurement shows little or no fluorescence recovery ( $R \ll 1$ ), indicating that the fluorescent molecules are not mobile in the time scale of the experiment.

### PEO diffusion as a function of temperature

The temperature dependence of  $D$  and  $R$  are shown in *Figure 2*. Above the melting temperature of PEO ( $T_m = 62^\circ\text{C}$ ), all the samples exhibited similar diffusional behaviour. The fluorescence recovery data can be fitted accurately to a theoretical curve describing the diffusion of a single component, and  $R$  is always 100%, indicating that fluorescent molecules in the probed area are completely mobile. In this temperature range the  $D$  values decreased monotonically with decreasing temperature. However, the rate of decrease in  $D$  is dependent on the concentration of added salts. The  $E_a$  of diffusion values

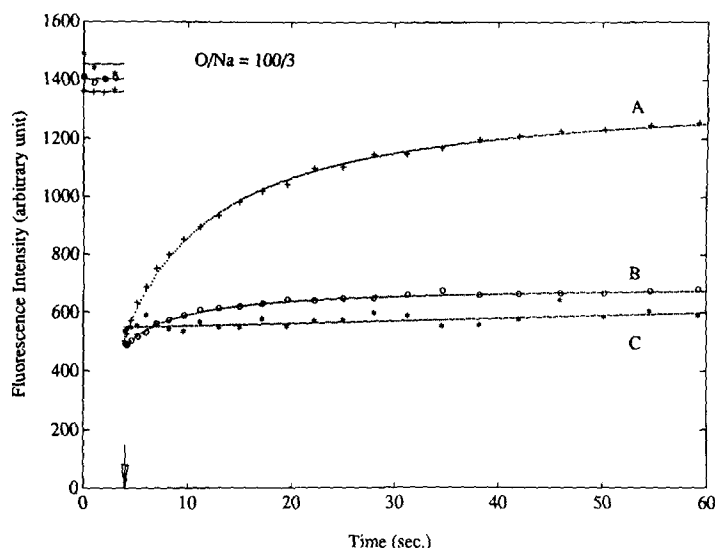


**Figure 1** Fluorescence recovery curves. Fluorescence intensity was monitored for 4 s, then at time  $t_b$  (marked by the arrow) a bright laser pulse is applied onto the sample for 5 ms to irreversibly bleach out some of the fluorophores. Following the photobleaching, fresh dye molecules diffuse into the probed area steadily raising the fluorescence intensity. Curve A (at 72°C) yielded  $D = 2.6 \times 10^{-9} \text{ cm}^2 \text{ s}^{-1}$  and  $R = 100\%$ . Curve B (at 60.5°C) yielded  $D = 1.9 \times 10^{-9} \text{ cm}^2 \text{ s}^{-1}$  and  $R = 37\%$ . For curves A and B the dotted lines are the theoretical curves. For curve C (at 52°C), data show little recovery, and the diffusion is too slow to measure (the dotted line is for illustration only and is not a theoretical curve)

for various samples were extracted from data in this temperature range. As the temperature approached 62°C, pure PEO samples started to form crystals, and the PEO diffusion essentially stopped, following the completion of crystallization. In the presence of NaI, samples usually crystallized at a lower temperature. The onset of crystallization, the rate of crystal growth, the crystal morphology and their dependence on  $D$  are different for each sample. Details will be published elsewhere. In the following, the self-diffusion of PEO for each studied concentration will be described.

**Pure PEO.** For samples made of pure PEO, the  $D$  value decreases with temperature, varying from  $D = 6.7 \times 10^{-9} \text{ cm}^2 \text{ s}^{-1}$  at 85°C to  $5.9 \times 10^{-9} \text{ cm}^2 \text{ s}^{-1}$  at 62°C (Figure 2a). Extrapolating the data to 100°C yielded a value  $D = 7.3 \times 10^{-9} \text{ cm}^2 \text{ s}^{-1}$ , which is in excellent agreement with the value reported by Sevreugin *et al.*<sup>30</sup> using the technique of pulsed field gradient n.m.r.

When the temperature was lowered to 62°C and held there for 15–20 min, pure PEO started to form visible (under microscope observation) crystals. This temperature is in agreement with the phase transition temperature,  $61 \pm 1^\circ\text{C}$ , observed in our d.s.c. measurements, and also the temperature reported by Chiang *et al.*<sup>31</sup>. Prior to the formation of visible crystals, the diffusional behaviour was similar to that observed at a higher temperature, namely, the sample appeared to be clear liquid, and the fluorescence recovery was almost 100% complete. Following the appearance of small nucleation clusters, the crystal grew rapidly. The growing edge of the spherulites advanced  $\sim 50 \mu\text{m min}^{-1}$ . During crystal growth, FRAP measurements yielded highly fluctuating results which were strongly dependent on the sample morphology.

In the regions without visible spherulites, PEO diffusion was fast and the fluorescence recovery was complete. Measurements made on the spherulites near the advancing growth edges resulted in only a slightly lower  $D$  value, but

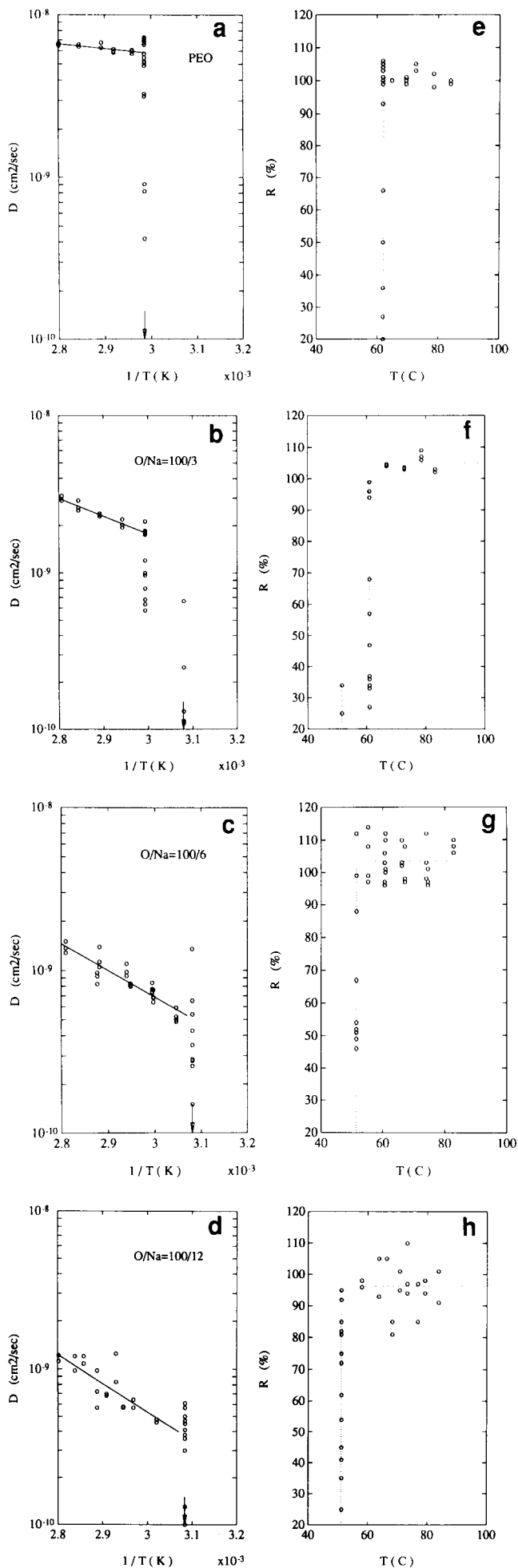
the fluorescence recovery was always  $< 100\%$ , suggesting that NBD-PEO still diffused at the same rate, but some of the PEO molecules were locked into the crystalline state and became immobile.

Measurements made near the centre of the spherulites, in most cases, resulted in slow diffusion and large immobile fractions (i.e.  $R \ll 1$ ). Following the completion of crystallization, which we define as the appearance of spherulites covering the whole sample, the diffusion essentially stopped. Occasionally, a slow diffusion process, with a large immobile fraction, could be detected in some areas, apparently due to unbound dye molecules or impurities.

At 62°C, both  $D$  and  $R$  values varied over a wide range (Figures 2a and e), reflecting the fluctuating results measured in various parts of the sample during the crystallization process. In addition, some of the results were unavoidably complicated by the continuing growth of crystals during the measurement. The arrow in Figure 2a (and also in Figures 2b–d) indicates that additional data with  $D$  values ranging from slightly less than  $10^{-10} \text{ cm}^2 \text{ s}^{-1}$  down to  $10^{-12} \text{ cm}^2 \text{ s}^{-1}$  are not displayed. The latter value is the practical measurable lower limit of our FRAP apparatus in this study.

**PEO sample with 3 mol% NaI.** Adding small amounts of salt to the system altered the crystal morphology and reduced the PEO diffusion rate significantly. In samples with 3 mol% NaI,  $D$  varied from  $3.0 \times 10^{-9} \text{ cm}^2 \text{ s}^{-1}$  at 85°C to  $1.8 \times 10^{-9} \text{ cm}^2 \text{ s}^{-1}$  at 62°C (Figure 2b). This  $D$  value is about three-fold lower than that found for pure PEO. No visible crystals were detected when the sample was held at 62°C (the melting temperature of pure PEO). FRAP measurements yielded high  $D$  values and complete fluorescence recovery after photobleaching. Such observation indicated that the melting temperature of PEO is depressed in the presence of salt.

When the temperature was brought to 60.5°C, no obvious morphological changes were initially noticed,



but after 30–40 min, some spherulite nuclei became visible, and crystals started to grow outwards from these nuclei. The rate of crystal growth was much slower than that for pure PEO at 62°C. The edges of the spherulites advanced  $< 1 \mu\text{m min}^{-1}$ . Most areas under investigation remained liquid-like up to several hours after the initial appearance of these spherulites. FRAP measurements made prior to the formation of crystals showed fast diffusion and complete fluorescence recovery, but after the appearance of crystals, measurements yielded fluctuating values in both  $D$  and  $R$ . In most cases, the PEO diffusion rate was high (albeit slightly lower than that at higher temperatures),  $D$  values vary within a factor of 4 only (Figure 2b), which is far less than the several orders of magnitude changes observed for pure PEO at 62°C (Figure 2a). However, the immobile fraction increased significantly (Figure 2f), indicating the presence of a new species in which PEO molecules were not mobile. All the measurements reported here were performed within an hour after the first appearance of crystals and on the regions without visible crystals.

When the sample temperature was lowered further to  $\sim 52^\circ\text{C}$ , the appearance of spherulites became very extensive, the diffusion slowed down rapidly and stopped after the completion of total crystallization. The fraction of fluorescence recovery was always  $< 40\%$ , indicating a large fraction of NBD-PEO was frozen in the immobile crystalline state.

**PEO samples with higher NaI concentrations.** PEO samples with 6, 9 and 12 mol% NaI exhibited similar diffusional behaviour. The value of  $D$  decreased monotonically with temperature. No significant change in  $D$  and  $R$  values were noticed near 62°C, the melting temperature for pure PEO, or near 60.5°C, the transition temperature for PEO samples with 3 mol% NaI. In addition, the sample morphology at these temperatures remained the same as at higher temperatures. For samples with 6 mol% NaI,  $D$  values varied from  $1.5 \times 10^{-9} \text{ cm}^2 \text{ s}^{-1}$  at 85°C to  $7.3 \times 10^{-10} \text{ cm}^2 \text{ s}^{-1}$  at 62°C (Figure 2c). These are about two-fold lower than the  $D$  values for 3 mol% NaI samples. Raising the concentration of NaI from 6 to 9 mol% decreased  $D$  only slightly (data for 9 mol% NaI are not shown) and further increase in salt concentration to 12 mol% resulted in little change in the  $D$  values. The concentration dependence of  $D$  values for two isotherms at 62°C and 85°C is shown in Figure 3.

As the temperature was lowered to  $\sim 52^\circ\text{C}$ , all the samples started to form visible crystals and the diffusion stopped following the completion of crystallization. Data reported here were measured within 2 h after the first appearance of crystals.

#### Phase diagram

Combining existing data from other laboratories with their results from microscope observations and conductivity measurements, Fauteux *et al.*<sup>14</sup> proposed a phase diagram for PEO and NaI mixtures. For the first time, the phase diagram of this well studied system was carefully mapped out. Our diffusion results provide

**Figure 2** Temperature dependence of  $D$  (a–d) and  $R$  (e–h). In a–d, the arrows indicate that data with  $D \leq 10^{-10} \text{ cm}^2 \text{ s}^{-1}$  are not shown. In e–h, the horizontal dotted line is the algebraic mean of the data (the vertical dotted line linking data points is for clarity)

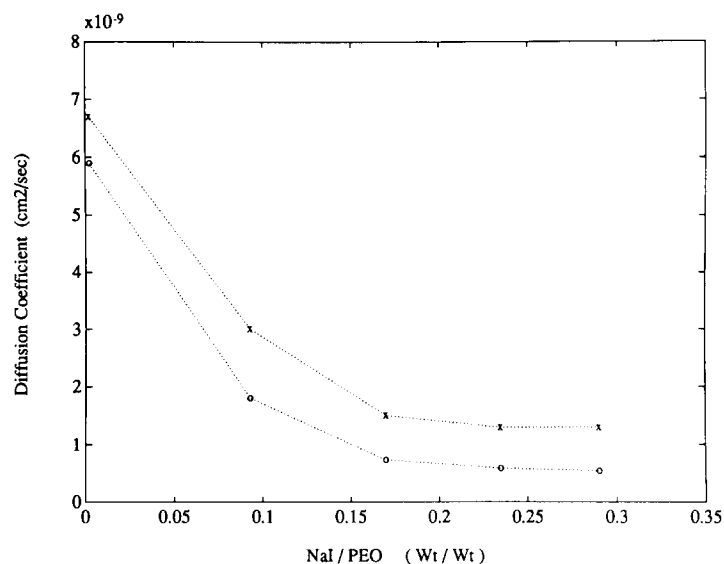


**Figure 3** Concentration dependence of the PEO self-diffusion coefficient at 62°C (○) and 85°C (×). *D* values were obtained from least-squares fitting. The *D* for pure PEO is shifted off the vertical axis slightly for clarity. Dotted lines linked the data points for easy visualization

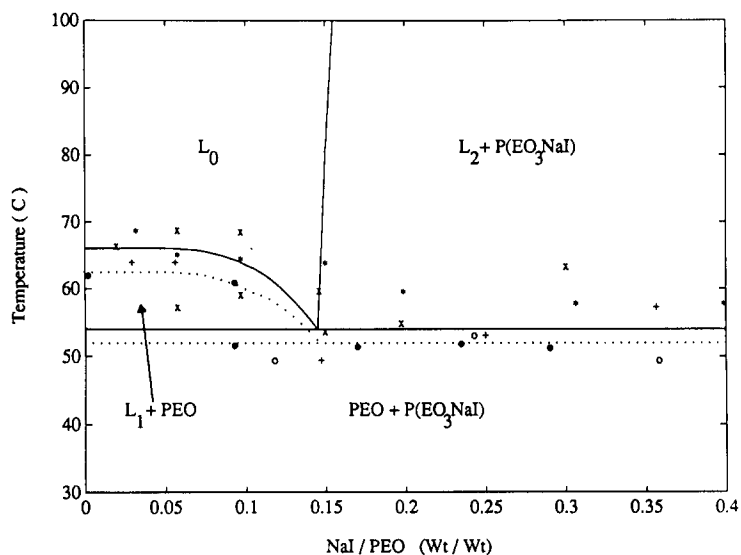


**Figure 4** Phase diagram for PEO and NaI mixtures. Dotted lines are the phase boundaries determined by the diffusion data (●) of this work. Solid curves represent the phase diagram proposed by Fauteux *et al.*<sup>14</sup>. Other data points were transferred from Figure 1 of reference 14. *L*<sub>0</sub>, *L*<sub>1</sub> and *L*<sub>2</sub> stand for various liquid-like amorphous phase compositions as explained in reference 14

further support for this diagram. For comparison, the transition points determined by our diffusion measurements are shown in *Figure 4* along with the data collected by Fauteux *et al.*<sup>14</sup>.

For pure PEO, *D* underwent a sharp change at 62°C, below which PEO is immobile and crystallized. This melting temperature is in good agreement with our d.s.c. results and those of Chiang *et al.*<sup>31</sup>. For samples with 3 mol% NaI, the *D* at high temperature is somewhat lower than that in pure PEO, suggesting that some PEO molecules complexed with NaI, and hence reduced the diffusion rate. At 60.5°C, the PEO *D* value exhibited large fluctuations and, most significantly, the amount of the immobile fraction started to increase (*Figure 2f*). This coincided with the appearance of small amounts of crystals in the system, indicating the onset of a new phase

in which crystalline PEO coexists with complexed PEO. Since FRAP measurements were performed in areas clear of visible crystals, the fluctuating values on *R* and *D* are apparently due to the presence of micro-crystals<sup>32,33</sup> that are smaller than the optical resolution (~1.5 μm) but sufficiently large to retard and freeze the mobility of PEO molecules. The measured *D* values are likely the weighted average of the *D* values due to complexed and crystallized PEO molecules. Using the notation of reference 14, this corresponds to the *L*<sub>1</sub> + PEO phase. A further sharp decrease in *D* was observed at 52°C, below which systems form solid phases and PEO self-diffusion stopped as observed in this study. This change is due to the transition across the eutectic reaction isotherm from the *L*<sub>1</sub> + PEO to the PEO + P(EO<sub>3</sub>NaI) phase.

Above 52°C, samples with 6, 9 and 12 mol% NaI

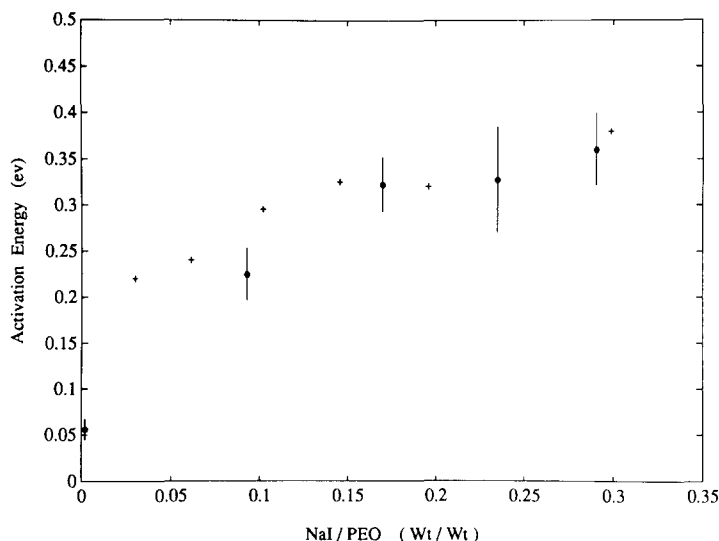


**Figure 5** NaI concentration dependence of the  $E_a$  of PEO self-diffusion (●) and the NaI concentration dependence of the  $E_a$  of ionic conductivity from reference 14 (+). For clarity, the  $E_a$  of PEO diffusion for pure PEO was shifted off the vertical axis slightly

formed various amounts of complexes with PEO, presumably in the form of the intermediate compound  $P(EO_3NaI)$ , which coexisted with liquid PEO. The  $D$  value and the mobile fraction changed only slightly in this temperature range. At 52°C a sharp drop in both  $D$  and  $R$  values were observed for all these samples as the electrolytes transformed to solid phases.

The phase boundaries suggested by our data (Figure 4, dotted lines) differ slightly from those proposed by Fauteux *et al.* (Figure 4, solid lines)<sup>14</sup>, probably due to the differences in PEO molecular weight and the thermal histories of the samples.

#### Self-diffusion coefficients

A careful analysis of molecular diffusion in crystalline or semicrystalline polymers requires detailed knowledge of the sample morphology and its thermal history<sup>34</sup>. This is beyond the scope of this paper. Instead, we direct our attention to the diffusion in regions above the melting temperature of PEO, where ionic conductivity is significant. In this region,  $D$  values decrease as the NaI concentration increases (Figure 3), and at a fixed NaI concentration, the  $D$  value increases with temperature (Figure 2). In the liquid state, PEO molecules are highly flexible and capable of interacting with many NaI molecules to form complexes<sup>1,35,36</sup>. Details of this interaction are not clearly known, but it is presumably due to the solvation of NaI by oxygen atoms in PEO molecules. The complexing of PEO with NaI in principle can be achieved by the association of  $Na^+$  with either inter- or intramolecular oxygen atoms. In the first case,  $Na^+$  is solvated by oxygen atoms from different PEO molecules. This intermolecular association may crosslink PEO molecules to form a transient network. (The network is transient because both  $Na^+$  and PEO are capable of diffusing over macroscopic distances.) Qualitatively, this is equivalent to the formation of extra entanglement nodes among PEO molecules or to the lengthening of the effective diffusion length of PEO<sup>18,37</sup>, and is expected to reduce the diffusion rate of PEO significantly. In the second case,  $Na^+$  is solvated by oxygen atoms from the same PEO molecule. Such

associations may alter the local conformation of PEO molecules, resulting in an increase in local viscosity, thus slowing down PEO diffusion. The observed diffusional behaviour is most likely affected by both inter- and intramolecular interactions. Since the extent of these interactions increases with the salt concentration,  $D$  is expected to decrease accordingly. Figure 3 shows the concentration dependence of the PEO  $D$  value for two isotherms. Both of them show that  $D$  decreases with the increase in salt concentrations.

#### Activation energy for diffusion

From the temperature dependence of  $D$ , the  $E_a$  of diffusion has been obtained by employing an Arrhenius-type relation.

$$D \propto \exp(-E_a/k_B T)$$

where  $k_B$  is Boltzmann's constant. Values of  $E_a$  of diffusion for five different samples, at temperatures above 52°C, are shown in Figure 5.  $E_a$  of diffusion increases with the NaI concentration.

Polymer self-diffusion has been interpreted in terms of free volume theory<sup>18,19</sup>, in which the temperature dependence of local viscosity is primarily coming from the free volume factor. The  $E_a$  of diffusion is essentially a measure of the local viscosity of the polymer chains. The increase of  $E_a$  of diffusion with NaI concentration reflects the increase of local viscosity in the polymer network in the presence of salt. Since ionic conduction is also a diffusion process, any changes in local viscosity that affect PEO diffusion will apparently affect the ionic conductivity to the same extent. This suggests that a similar concentration dependence in  $E_a$  of diffusion should be observed for the  $E_a$  of ionic conductivity. Fauteux *et al.* have measured the apparent  $E_a$  of ionic conductivity as a function of NaI concentrations<sup>14</sup>, and found that, in the concentration range covered in this work, their  $E_a$  also increased with NaI concentration. As a comparison, we have plotted their  $E_a$  for ionic diffusion in Figure 5. Within the experimental uncertainties, the agreement between these two  $E_a$  values is reasonably good. Killis *et al.*<sup>9</sup> correlated the ionic conductivity and

the dynamic mechanical properties of a crosslinked polymer network and concluded that mobile ions and chain segments share the same free volume fraction for their diffusion; this conclusion is in accord with our observation.

## CONCLUSIONS

Using the technique of FRAP we have measured the  $D$  values of PEO in NaI-PEO electrolytes. The interactions of PEO with  $\text{Na}^+$  retarded the diffusion of PEO significantly, possibly due to the formation of a transient network which has the same effect as entanglement on polymer self-diffusion. From the temperature dependence of  $D$ , the  $E_a$  of diffusion was obtained. It has the same salt concentration dependence as the  $E_a$  of ionic conductivity. This strongly suggests that polymer segmental mobility is essential for ion transport in NaI-PEO electrolytes.

## ACKNOWLEDGEMENTS

We thank Dr G. T. Davis for helpful discussions, Dr A. Y. Wu for the computer curve fitting and graphic display, and the Academic Computing Services at UMBC for providing the computer time.

## REFERENCES

- 1 Cowie, J. M. G. and Cree, S. H. *Ann. Rev. Phys. Chem.* 1989, **113**, 85
- 2 Vincent, C. A. *Prog. Solid State Chem.* 1987, **17**, 145
- 3 Armand, M. B. *Ann. Rev. Mater. Sci.* 1986, **16**, 245
- 4 Armand, M. B., Chabagno, J. N. and Duclot, M. J. 'Fast Ion Transport in Solids, Electrodes and Electrolytes' (Eds P. Vashishta, J. M. Mundy and G. K. Shenoy), North Holland, New York, 1979, p. 131
- 5 Rapke, B. L., Ratner, M. A. and Shriver, D. F. *J. Electrochem. Soc.* 1982, **129**, 1694
- 6 MacCallum, J. R., Tomlin, A. S. and Vincent, C. A. *Eur. Polym. J.* 1986, **22**, 787
- 7 Wintersgill, M. C., Fontanella, J. J., Pak, Y. S., Greenbaum, S. G., Al-Mudaris, A. and Chadwick, A. V. *Polymer* 1989, **30**, 1123
- 8 Cameron, G. G., Ingram, M. D. and Sorrie, G. A. *J. Chem. Soc., Faraday Trans.* 1987, **83**, 3343
- 9 Killis, A., Le Nest, J. F., Gandini, A., Cheradame, H. and Cohen-Addad, J. P. *Solid State Ionics* 1984, **14**, 231
- 10 Minier, M., Berthier, C. and Gorecki, W. *J. Phys.* 1984, **45**, 739
- 11 Greenbaum, S. G., Pak, Y. S., Wintersgill, W. C., Fontanella, J. J., Schultz, J. W. and Andeen, C. G. *J. Electrochem. Soc.* 1988, **135**, 235
- 12 Minier, M., Berthier, C., Gorecki, W. J., Armand, M. B., Chabagno, J. M. and Rigaud, P. *Solid State Ionics* 1983, **11**, 91
- 13 Sassabe, H. and Saito, S. *Polym. J.* 1972, **3**, 624
- 14 Fauteux, C. D., Lupien, M. D. and Robitaille, C. D. *J. Electrochem. Soc.* 1987, **134**, 2761
- 15 Gorecki, W., Andreani, R., Berthier, C., Armand, M., Mali, M., Roos, J. and Brinkmann, D. *Solid State Ionics* 1986, **18/19**, 295
- 16 Robitaille, C. D. and Fauteux, D. *J. Electrochem. Soc.* 1986, **133**, 315
- 17 Ferloni, P., Chiodelli, G., Magistris, A. and Sanesi, M. *Solid State Ionics* 1986, **18/19**, 265
- 18 Vrentas, J. S., Duda, J. L. and Ni, L.-W. *Macromolecules* 1983, **16**, 261
- 19 Vrentas, J. S. and Duda, J. L. *J. Polym. Sci., Polym. Phys. Edn.* 1979, **17**, 1085
- 20 De Gennes, P.-G. 'Scaling Concepts in Polymer Physics', Cornell University Press, Ithaca, 1979
- 21 Tirrell, M. *Rubber Chem. Technol.* 1984, **57**, 523
- 22 Druger, D. S., Ratner, M. A. and Nitzen, A. *Phys. Rev. B* 1985, **31**, 3939
- 23 Druger, D. S., Nitzen, A. and Ratner, M. A. *J. Chem. Phys.* 1983, **79**, 3133
- 24 Lodge, A. *Trans. Faraday Soc.* 1956, **52**, 120
- 25 Ronca, G. *Rheol. Acta* 1976, **15**, 149
- 26 Wu, E. S., Jacobson, K., Szoka, F. and Portis, A. *Biochemistry* 1978, **17**, 5543
- 27 Wang, F. W., Lowry, R. E. and Wu, E. S. *Polymer* 1985, **26**, 1654
- 28 Axelrod, D., Koppel, D. E., Schlessinger, J., Elson, E. and Webb, W. W. *Biophys. J.* 1976, **16**, 1055
- 29 Cuniiberti, C. and Perico, A. *Eur. Polym. J.* 1977, **13**, 369
- 30 Sevreguin, V. A., Skirda, V. D. and Maklakov, A. I. *Polymer* 1986, **27**, 290
- 31 Chiang, C. K., Davis, G. T., Harding, A. and Aarons, J. *Solid State Ionics* 1983, **9/10**, 1121
- 32 Hoffman, J. D., Frolen, L. J., Ross, G. S. and Lauritzen, J. I. *J. Res. Natl Bur. Stand.* 1975, **A79**, 671
- 33 Chew, S., Griffiths, J. R. and Stachurski, Z. H. *Polymer* 1989, **30**, 874
- 34 Klein, J. and Briscoe, B. J. *Proc. R. Soc. Lond. [A]* 1979, **365**, 53; Klein, J. *J. Polym. Sci., Polym. Phys. Edn.* 1977, **15**, 2057
- 35 Chatani, Y. and Okamura, S. *Polymer* 1987, **28**, 1815
- 36 Hibma, T. *Solid State Ionics* 1983, **9/10**, 1101
- 37 Bueche, F. 'Physical Properties of Polymers', Interscience, New York, 1962